



UNIVERSITY OF LEEDS

This is a repository copy of *Multiscale investigation on the cement-lime modified red mudstone as fill material for high-speed railway*.

White Rose Research Online URL for this paper:

<https://eprints.whiterose.ac.uk/id/eprint/231460/>

Version: Accepted Version

Article:

Xu, J., Liu, X., Yuan, S. et al. (5 more authors) (2025) Multiscale investigation on the cement-lime modified red mudstone as fill material for high-speed railway. *Bulletin of Engineering Geology and the Environment*, 84. 309. ISSN: 1435-9529

<https://doi.org/10.1007/s10064-025-04337-5>

This is an author produced version of an article published in *Bulletin of Engineering Geology and the Environment*, made available under the terms of the Creative Commons Attribution License (CC-BY), which permits unrestricted use, distribution and reproduction in any medium, provided the original work is properly cited.

Reuse

This article is distributed under the terms of the Creative Commons Attribution (CC BY) licence. This licence allows you to distribute, remix, tweak, and build upon the work, even commercially, as long as you credit the authors for the original work. More information and the full terms of the licence here:

<https://creativecommons.org/licenses/>

Takedown

If you consider content in White Rose Research Online to be in breach of UK law, please notify us by emailing eprints@whiterose.ac.uk including the URL of the record and the reason for the withdrawal request.



eprints@whiterose.ac.uk
<https://eprints.whiterose.ac.uk/>

Multiscale investigation on the cement-lime modified red mudstone as fill material for high-speed railway

Jiahang Xu^{2,3,4}, Xianfeng Liu^{1,2}, Shengyang Yuan^{1,2}, Jie Ma^{1,2}, Dariusz Wanatowski^{3,4}, Ana Heitor⁴, Ren Hu^{1,2}, Feng Chen⁵

¹ Department of Civil Engineering, Southwest Jiaotong University, 111 Second Ring Road of North Section 1, Chengdu, Sichuan Province, China

² Key Laboratory of High-Speed Railway Engineering, Ministry of Education, 111 Second Ring Road of North Section 1, Chengdu, Sichuan Province, China

³ Leeds Joint School, Southwest Jiaotong University, 111 Second Ring Road of North Section 1, Chengdu, Sichuan Province, China

⁴ Faculty of Engineering and Physical Sciences, University of Leeds, Leeds, LS2 9JT, UK

⁵ Railway Engineering Research Institute, China Academy of Railway Sciences Co., Ltd, Beijing, China

Corresponding author: Xianfeng.liu@swjtu.edu.cn

Statements and Declarations

Funding

Partial financial support was received from Natural Science Foundation of China (No. 52008355, No. 52078432 and No. 52478475) and the funding of China Academy of Railway Science Group Co., LTD (NO. 2023YJ377)

Competing interests

The authors have no relevant financial or non-financial interests to disclose.

Abstract.

The construction of high-speed railway in Southwest China must traverse extensive regions of red mudstone. However, due to the humid subtropical monsoon climate in Southwest region, the red mudstone is often exposed to a high-water content or saturated state for extended time, and the poor mechanical properties under such condition cannot satisfy the requirements of high-speed railway subgrade. This paper proposes the use of lime and cement to improve the saturated unconfined compression strength (UCS) of the red mudstone fill material. Comprehensive tests, including UCS tests and scanning electron microscopy, were conducted on cement-lime modified red mudstone. Results show that lime stabilisation can significantly enhance the UCS and elastic modulus with the increase of dry density and modifier content. For the specimens with 4% lime and 6% cement, both peak strength and elastic modulus of the modified samples are more than 10 times higher than those of the untreated ones. The modulus exhibits nonlinear degradation with the development of shear stress, but the degradation can be improved with the increase of dry density and modifier content. At 60% of initial tangent modulus, the corresponding stress for untreated soil, lime stabilised and cement-lime modified filler are 0.74, 0.92 and 0.99. As for the energy evolution, the increasing dry density can enhance elastic and dissipated energies through denser particle arrangements, while a higher modifier content raises total energy. When the cement content is 6%, the total energy is more than 8 times higher than that of the untreated material, reflecting increased brittleness to a sudden fracture. The improvements are attributed to the formation of acicular and platy hydration products, which can tighten the pore structure. The study underscores the importance of lime and cement in ensuring subgrade stability for high-speed railways in Southwest China's red bed regions.

Key words: High-speed railway subgrade fill material, lime stabilisation, cement-lime modification, UCS, SEM

1. Introduction

Red mudstone, widely distributed in Southwest China, poses significant challenges for railways and other types of infrastructure due to its weak mechanical properties(Zhang et al. 2016, 2018; Xu et al. 2024b). According to the national policy, the vast of existing and intended railway lines must inevitably pass through the red bed region. In parallel, the fill material of the high-speed railway is required to fall within group A and B, as specified by the Code for Design of High Speed Railway (TB 10621-2014) (Ministry of Railways of the People's Republic of China 2015). However, fully weathered red mudstone falls into Group C due to its high fine particle content requirements(China Railway First Survey and Design Institute Group Co., Ltd. 2005; Chen et al. 2014, 2022; Xu et al. 2024a). Nevertheless, due to the mountainous topography of Southwest region, the transportation of the high-quality fill material is restricted which may lead to a significant increase in investment. Besides, the improper disposition of the red mudstone waste might cause environmental pollution or even trigger secondary disasters. Therefore, there is a clear and pressing need to utilise red mudstone waste as subgrade fill material for high-speed railways.

So far, red mudstone has been used as the fill material for the highway and the conventional railway. However, poor mechanical properties and high water sensitivity may lead to cracks, uneven settlement and collapse of the subgrade. Therefore, the modification is required before subgrade construction. Generally, the modification strategy for high-speed railway subgrade fill material still follows the relevant methods used in conventional railway, including mixing the lime, cement and fly ash with the filler, which can mitigate the water sensitivity and enhance the strength. Jiang (Wang et al. 2008, 2010; Zhan et al. 2009; Hu et al. 2010; Kong et al. 2013) has complemented site dynamic investigation of the lime stabilised red mudstone fill material in Da-cheng and Sui-yu railway lines. The results indicate that the water sensitivity was significantly improved and the stabilised filler could satisfy the requirement of bottom layer of 200km/h railway subgrade(Al-Mukhtar et al. 2010; Aldaood et al. 2014; Maubec et al. 2017; GhavamShirazi and Bilsel 2021). Other studies have shown that the addition of

cement could further enhance the strength and modulus of the soil to a greater extent (Wang et al. 2023b; Wassie and Demir 2024; Ayers et al. 2024; Onyelowe et al. 2024). Some other studies also focused on the energy evolution of the modified soil (Wang et al. 2023a; Huang et al. 2023). Moreover, several researchers have also carried out macroscopic and microscopic laboratory tests on the modified fill materials. The hydration products of lime and cement including Calcium Aluminate Hydrates and Calcium Alumino-Silicate Hydrates could fill within the soil particles and adhere them together (Alvarez et al. 2013; Tran et al. 2014; Wang et al. 2015).

As the designed operating speeds of high-speed trains increase, the subgrade would be subject to more stringent requirements. While the addition of lime can improve the strength characteristics of red mudstone fill material, cement addition would lead to even more significant enhancements. Although some research has been conducted on lime-stabilised red mudstone fill material, studies on the mechanical properties of cement-lime modified fill material remain limited, and the quantitative comparisons before and after modification are not clear. This study intends to fill this gap at both macro- and micro- scales.

In this study, a series of unconfined compression strength (UCS) tests under different initial dry densities and modifier contents were implemented on the saturated red mudstone fill material, lime stabilised and cement-lime modified fill materials. The study was completed by microstructural analysis using scanning electron microscopy. The results are initially discussed from the viewpoint of strength and energy. The modification mechanism was then analysed considering the coupling among the soil particles and the hydration product of the cement-lime. The results provide valuable insights for addressing subgrade stability challenges in red bed regions of Southwest China with the addition of lime and cement, directly supporting the acceleration of high-speed railway.

2. Materials

A fully weathered red mudstone used for the experiments was sourced from Tianfu district in Chengdu, China. After pre-disintegration and hammer crushing, the particles

with a diameter smaller than 1mm were chosen as the testing material. The particle size distribution of the red mudstone was thoroughly measured using a Malvern laser particle size analyser. The resulting distribution curve (as shown in Fig. 1(a)) clearly indicates that the coefficient of uniformity C_u is equal to 6, and the coefficient of curvature C_c is equal to 1.5. To further understand the physical properties of the red mudstone, the standard proctor compaction test (Fig. 1(b)) was conducted, determining the maximum dry density (ρ_{dmax}) of 1.77 g/cm³ and the optimum water content (w_{opt}) of 16.3%. Additionally, X-ray diffraction (XRD) analysis was performed and the results (as shown in Fig. 2) indicate that the red mudstone consists of multiple minerals, primarily including calcite, quartz, muscovite, montmorillonite, and albite. The basic physical properties of red mudstone are shown in Table 1.

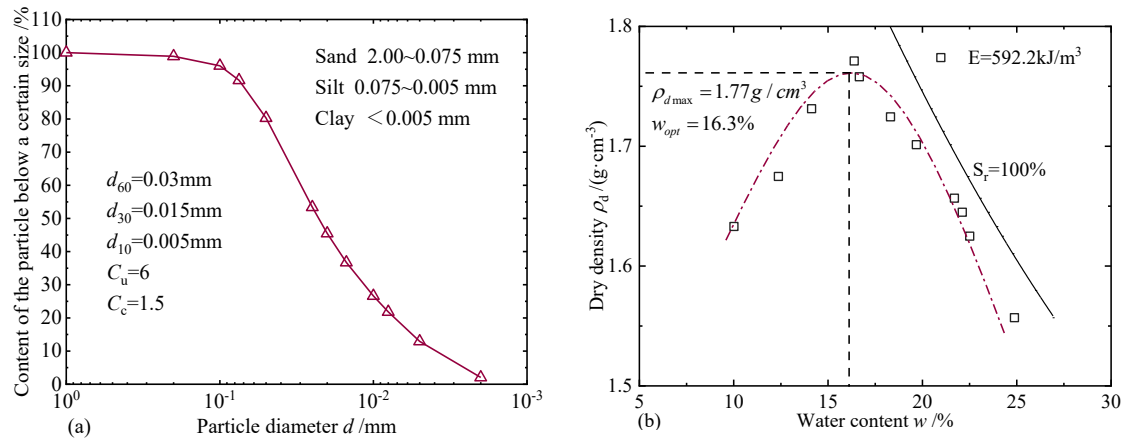


Fig. 1 (a) Particle distribution curve (b) Compaction curve

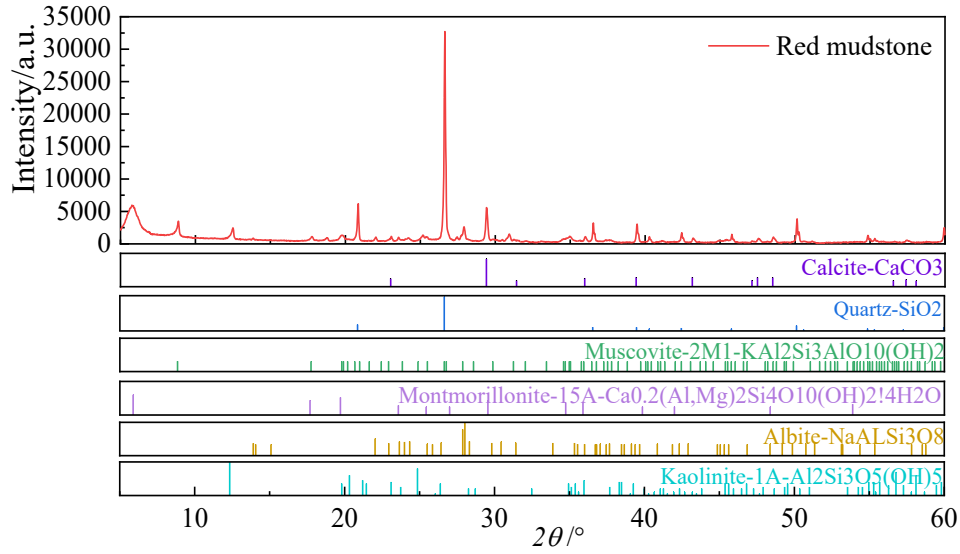


Fig. 1 X-ray diffraction pattern of red mudstone

Table 1. Physical and mechanical parameters of red mudstone.

Maximum dry density /($\text{g}\cdot\text{cm}^{-3}$)	Optimal water content /%	Liquid limit /%	Plastic Limit /%	Specific gravity
1.77	16.3	32.5	13.8	2.69

Portland cement of grade 42.5, the most common type used in civil engineering construction, was selected for stabilisation. The lime used in the test was Grade I quicklime with a CaO content of more than 87% and a particle size of less than 1 mm. The basic physical properties of this type of lime matched with previous research (Liu et al. 2024; Ma et al. 2024), allowing for systematic comparison of the results from this study with past findings.

3. Experimental programme and methods

According to Code for Design of High Speed Railway (TB10621-2014), the compaction coefficient of modified soil should be no less than 0.95, and the UCS for saturated soil with curing age of 7 days should be no less than 350kPa to meet the demands of accelerating high-speed railway. A series of UCS tests were performed to obtain the static response of red mudstone, lime stabilised red mudstone and cement-lime modified red mudstone, as shown in Table 2.

The tests were designed to analyse the effects of initial dry density and modifier content. In terms of the effect of dry density, based on the compaction test ($\rho_{\text{dmax}}=1.77$

g/cm³) and the requirement of the design code ($K \geq 0.95$), the initial dry densities were set as 1.6, 1.7, 1.8 and 1.9 g/cm³ and were applied to both red mudstone fill material and the modified fillers so that the effect of dry density could be determined. Taking $\rho_d = 1.7$ g/cm³ as the standard dry density, different contents of lime (0, 2, 4, 6 and 8%) were used so that the effects of initial dry density and lime content on the UCS of lime stabilised red mudstone could be analysed. According to the site investigation and several years of operation in Da-cheng and Sui-yu railway lines, the optimum lime content was determined as 4%. On this basis, the cement contents of 0, 2, 4 and 6% were applied so that the effect of cement content could be clarified. Furthermore, early strength characteristics are more beneficial to meet the construction and operational requirements of the subgrade. Thus, the tests were carried out after 7 days of curing and the loading rate was 0.128mm/min. To reveal the modification mechanisms, SEM analysis was performed on the red mudstone fill material before and after saturation, as well as on the modified filler under saturation state.

Note that all the tests were conducted based on Code for Soil Test of Railway Engineering (TB 10102-2023)(China Railway First Survey and Design Institute Group Co., LTD et al. 2023). The red mudstone used in the experiment was dried in an oven to 105°C, then sprayed evenly with water to reach the target water content, and finally sealed in a vacuum bag to achieve water equilibrium for 24 hours. By precisely controlling the loading rate of 1 mm/min, the mudstone was statically pressed into cylindrical samples with a diameter of 38 mm and a height of 76 mm, compacted in five layers, and then vacuum-sealed again for UCS testing. Meanwhile, the specimens for the SEM test were first freeze-dried for 48 hours and then coated with gold (Au). The SEM analysis was conducted using a JSM-IT500 apparatus.

The testing process is shown in Fig. 3.

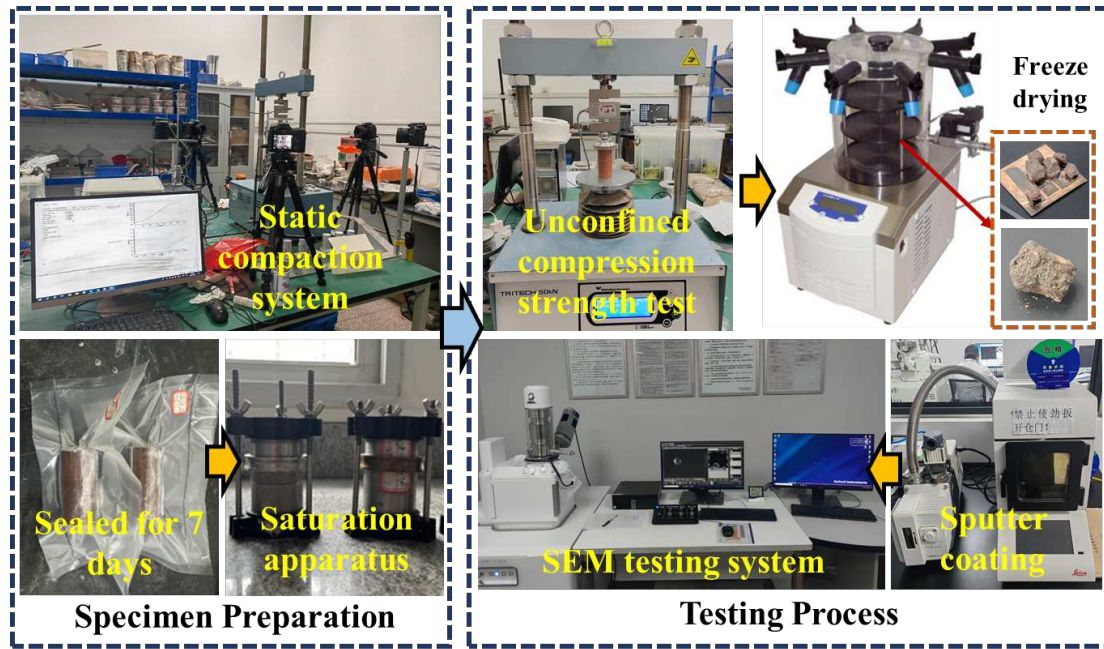


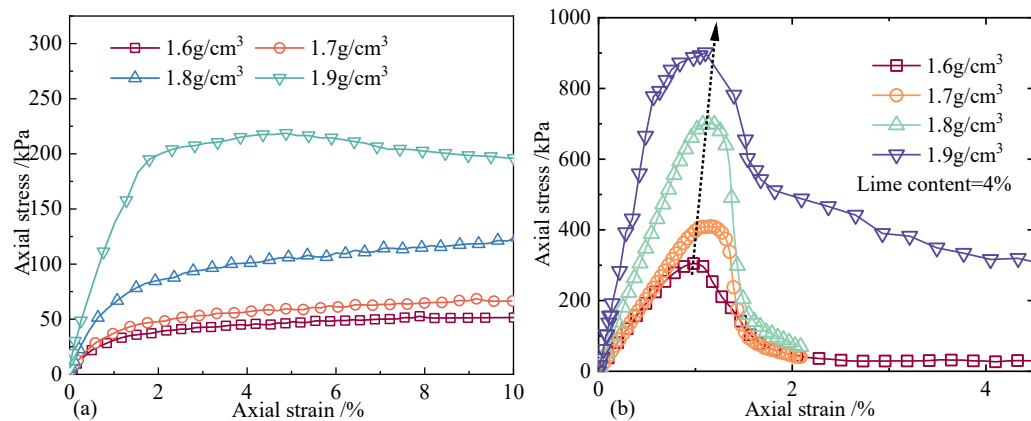
Fig. 2 Illustration of testing procedures

Table 2. Unconfined compression strength test programmes.

Water content /%	Dry density / $\text{g}\cdot\text{cm}^{-3}$	Lime content /%	Cement content /% (with 4% lime)
Sat	1.6	0, 4	2
	1.7	0, 2, 4, 6, 8	0, 2, 4, 6
	1.8	0, 4	2
	1.9	0, 4	2

4. Results and discussion

4.1 The effect of the dry density on the strength characteristics



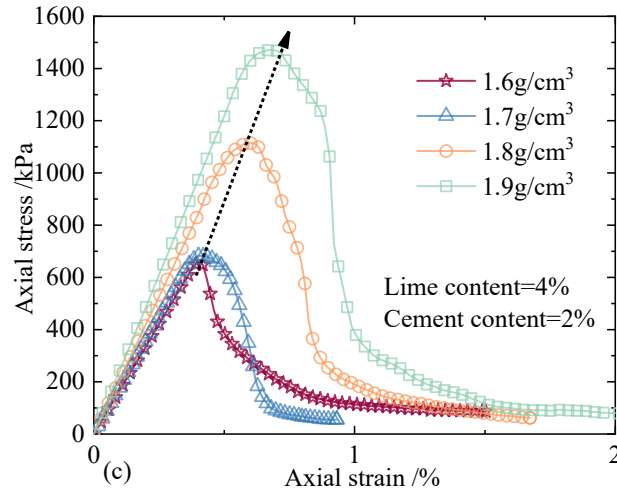


Fig. 3 Stress-strain curves of (a) Red mudstone with different dry densities (b) Lime stabilised red mudstone with different dry densities (c) Cement-lime modified red mudstone with different dry densities

Fig. 4 illustrates the effect of initial dry density on the stress-strain behaviour of the saturated red mudstone before and after modification. According to Fig. 4 (a), the axial stress of the untreated fill material shows a linear upward tendency at the beginning of the shearing. With the increase of the strain, the cracks within the specimens started to evolve which could lead to the deterioration of the deformation resistance. The increasing rate of the axial stress decreased when reaching the peak value. The stress-strain curves displayed a hardening behaviour. However, for the modified filler shown in Fig. 4 (b) and (c), the shearing behaviour turn from hardening to softening and the failure mode shows a more brittle trend after adding lime and cement. Meanwhile, with the increase of the dry density, the axial strain corresponding to the peak strength would increase.

Fig. 5 (a) and (b) demonstrate the influence of initial dry density on the peak strength as well as the elastic modulus. It could be observed that the larger the dry density, the larger the peak stress and the elastic modulus. Both strength and modulus are significantly improved after modification, especially for cement-lime modified red mudstone fill material. Moreover, the increase of the elastic modulus also reflects the increase of the brittleness.

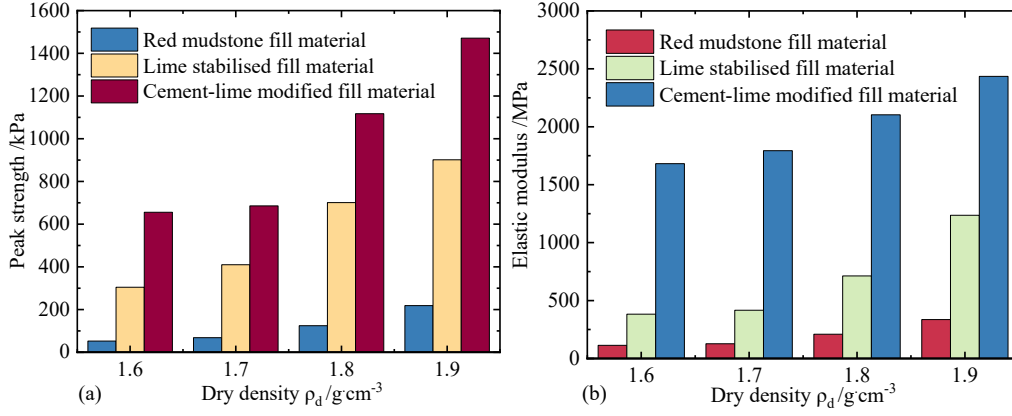


Fig. 4 (a) Evolution of the peak strength with different dry density before and after modification (b) Evolution of elastic modulus with different dry density before and after modification

The structural damage of the red mudstone could be described as the production of energy evolution. From a macro-scale perspective, this damage process could be quantified by the deterioration of the tangent modulus. Herein, the normalised modulus E_{nor} and the strength criteria q_{nor} could be defined as:

$$E_{nor} = \frac{E_{tan}}{E_i} \quad (1)$$

$$q_{nor} = \frac{q}{q_{max}} \quad (2)$$

where q_{max} is the peak strength and E_i is the elastic modulus. To ensure the safety of the high-speed railway, the strength failure of the subgrade is strictly forbidden. Therefore, the analysis presented in this paper only focuses on the shearing process before reaching the peak strength, that is pre-peak behaviour.

Fig. 6 shows the effect of dry density on the normalised modulus under saturated state. In terms of the untreated fill materials, the modulus shows a nonlinear tendency with the development of the stress. The deterioration trend appears at the beginning of the shear and becomes more obvious until it reaches the peak strength. During this process, the smaller the dry density, the faster the deterioration. As shown in Fig. 6, when $E_{nor} = 0.6$, the q_{nor} of 1.9 g/cm^3 is still larger than 85%, while the values for 1.6, 1.7 and 1.8 g/cm^3 are 66%, 72% and 75%, respectively. This quantifies the stress required to degrade the modulus of fill material to a predetermined extent. A higher dry density enhances the fill material's capacity to withstand external loads. For red

mudstone subgrade, once the specified compaction degree and dry density could not be reached, even a relatively small shear stress can rapidly diminish the bearing capacity. Although the stress level is not high enough to directly cause the immediate failure of the subgrade, it is sufficient to cause significant deterioration, which may induce the deformation or settlement of the subgrade, and ultimately lead to irregularity of the line.

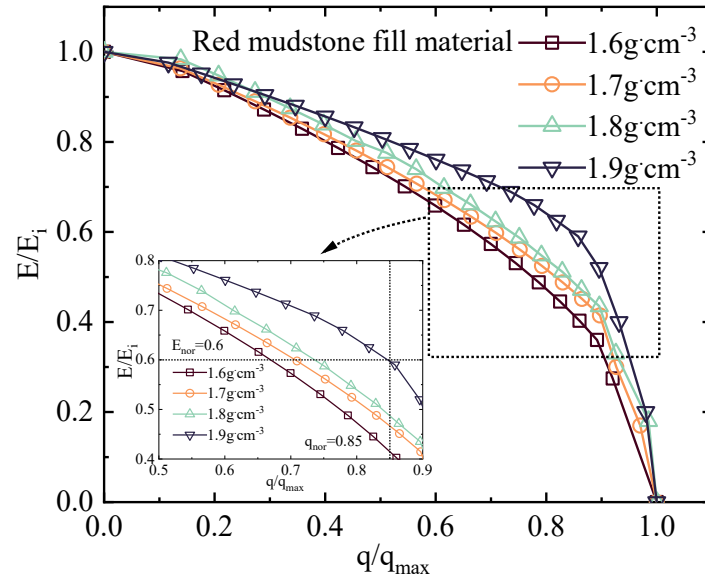


Fig. 5 Effect of dry density on deterioration of normalised modulus of red mudstone fill material

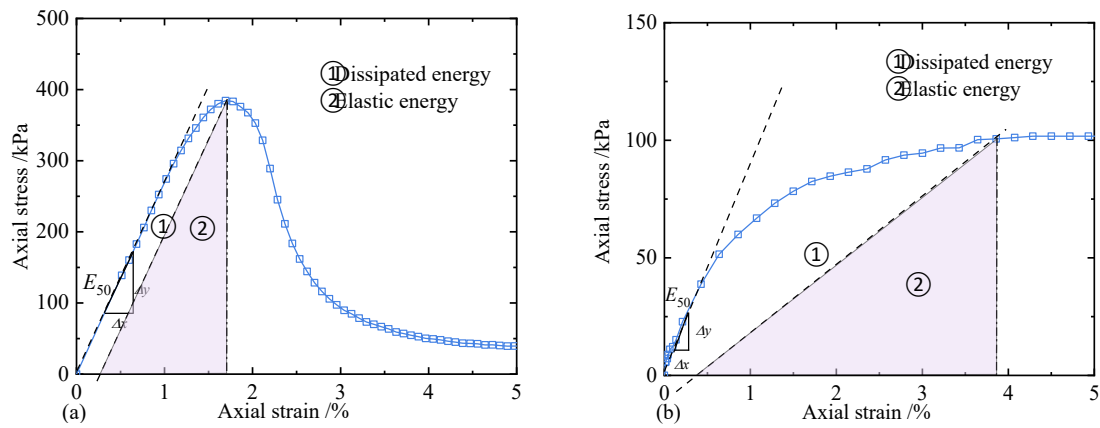


Fig. 6 Diagrams of dissipative energy and elastic energy (a) Softening (b) Hardening

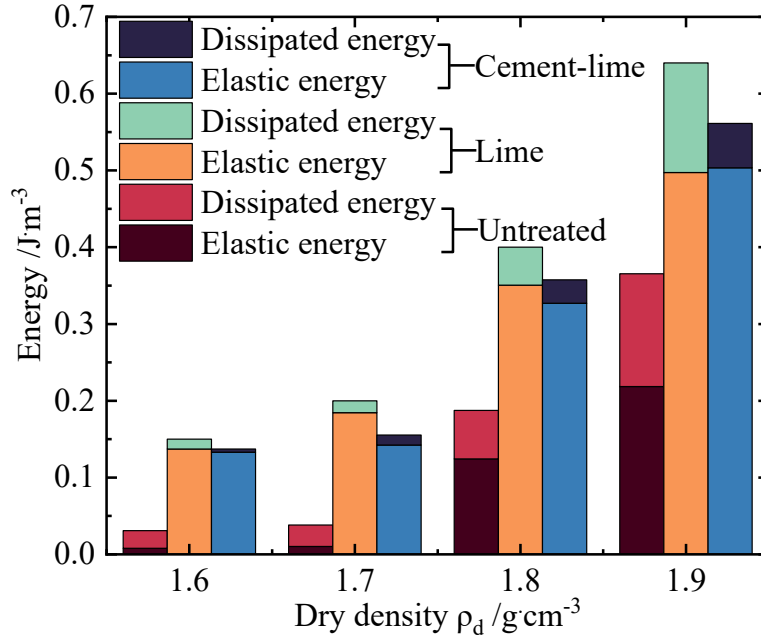


Fig. 7 Evolution of energy with different dry density before and after modification

Herein, researches have shown that the mechanical performance can be explained via energy evolution (Chen et al. 2023). During the shearing process, the elastic energy indicates the recovery ability of the specimen structure. Nevertheless, if the proportion of dissipated energy increases, the specimen suffers larger degree of irreversible damage which in turn reduces the loading resistance of the specimen. Fig. 7 presents the schematic illustrations of dissipated and elastic energy.

Fig. 8 illustrates the evolution of energy with different dry densities before and after modification. With the increase of dry density, both two parts of energy show upward trend. This is because the closer arrangement of the soil particles could enhance the strength, and the energy would be dissipated via occlusion as well as friction. It is also interesting to find that the total energy of the cement-lime modified red mudstone fill material (cement 2%, lime 4%) is less than the lime stabilised one (lime 4%). It can be observed that although the peak strength of the former one is much larger, the axial strain corresponding to the peak strength is becoming smaller. This could also indicate that the addition of cement brings the specimen to a more brittle behaviour which could demonstrate more clearly the brittle failure mentioned above.

4.2 The effect of the modifier content on the strength characteristics

Fig. 9 presents the effect of modifier content on the stress-strain behaviour of the stabilised red mudstone. It can be observed that the UCS of the lime stabilised filler is significantly improved, yet the growth rate of the strength is decreasing (Fig. 9 (a)). In terms of cement-lime modified filler, the axial strain corresponding to the peak strength is smaller, and the value becomes larger with the increase of the cement content. This could also reflect the increase of the brittleness of the cement-lime stabilised specimens. It should be noted that for the specimens with different cement contents, take L4C2 for instance, the test number refers to the cement-lime modified red mudstone with a lime content of 4% and cement content of 2%. In addition, Fig. 10 shows the influence of modifier content on the peak strength and elastic modulus of the red mudstone. The peak strength and elastic modulus increase linearly with the increase of modifier content. The peak strength and the elastic modulus of the stabilised red mudstone are more than 10 times than those of the untreated fill material.

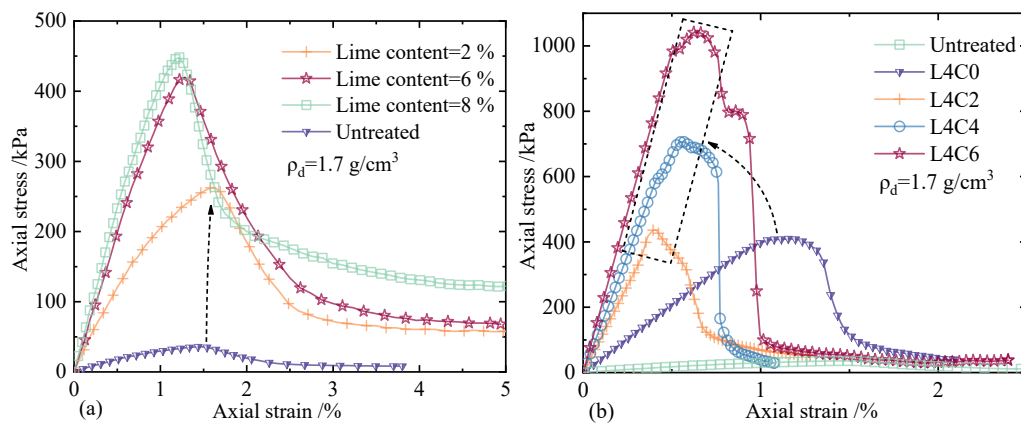


Fig. 8 Stress-strain curves of (a) Lime stabilised red mudstone with different lime content (b) Cement-lime modified red mudstone with different cement content

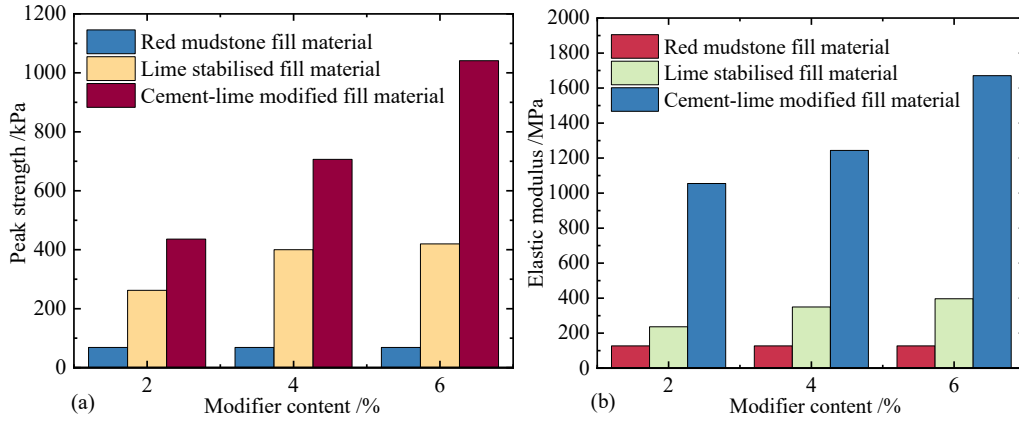


Fig. 9 (a) Evolution of peak strength with different modifier content before and after modification (b) Evolution of elastic modulus with different modifier content before and after modification

Fig. 11 illustrates the effect of modifier content on the deterioration law of the normalised modulus with stress development under saturated state. When the modulus decays to 60%, that is, when E_{nor} is 0.6, the q_{nor} of the lime stabilised filler (2% lime) is greater than 0.8, while the value of the untreated one is 0.72. Moreover, with the increase of lime content (4% and 6%), the q_{nor} for these two states would be 0.91 and 0.99, respectively. This indicates that the addition of lime can increase the requisite normalised stress when the modulus deteriorates to 60%. In other words, the modification can greatly inhibit the deterioration due to water immersion of red mudstone, and the higher the lime content, the more obvious this phenomenon. In parallel, as shown in Fig. 12, the modulus deterioration evolution of cement-lime modified filler is similar to this.

The results of modulus deterioration of untreated red mudstone fill material and the two modified fillers are compared in Fig. 12. When the tangent modulus of the filler decreases to 60% of the initial value, the corresponding shear stress levels of the untreated soil, lime stabilised and cement-lime modified filler are 0.74, 0.92 and 0.99, respectively, which indicates that the addition of modifier could boost the fill material ability to withstand external loads. Moreover, it can be observed that the modulus begins to deteriorate at a low stress for the untreated red mudstone, while the stress for “starting point of modulus deterioration” of modified filler is much larger. The effects

are more evident in the cement-lime modified fill materials than in the lime stabilised ones.

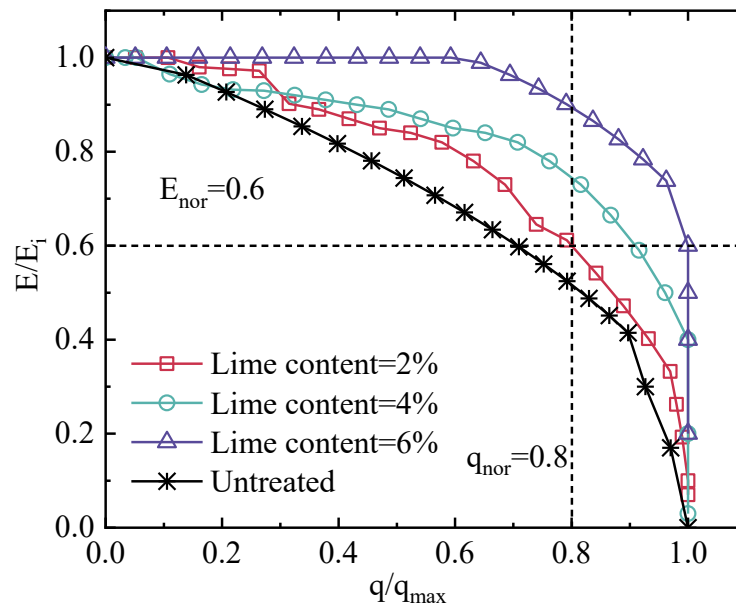


Fig. 10 Effect of modifier content on deterioration of normalised modulus of red mudstone fill material

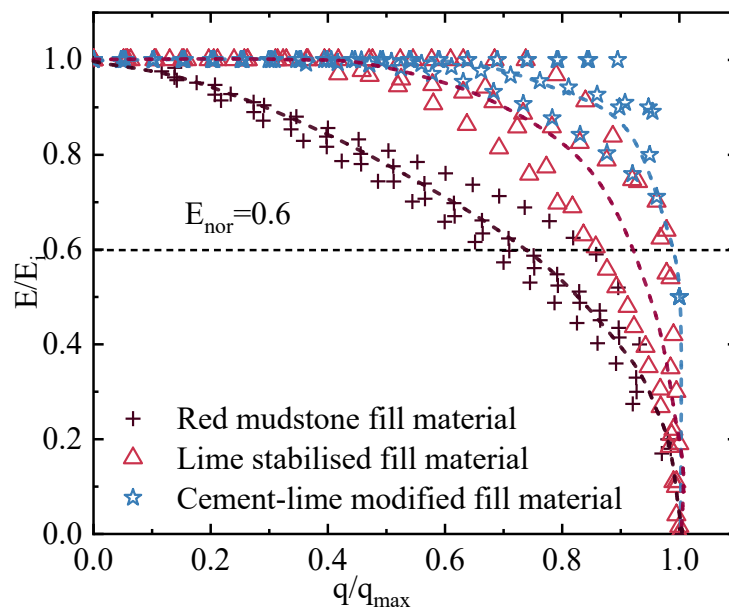


Fig. 11 Normalised modulus degradation curves of fill material before and after modification

Fig. 13 shows the changes of dissipative energy and elastic energy with the modifier content. With the increase of lime content, the elastic energy and dissipative energy increase slightly. As for cement-lime modified fillers, with the increase of cement

content, the total energy and the energy of each component increased significantly, and the brittleness was more obvious.

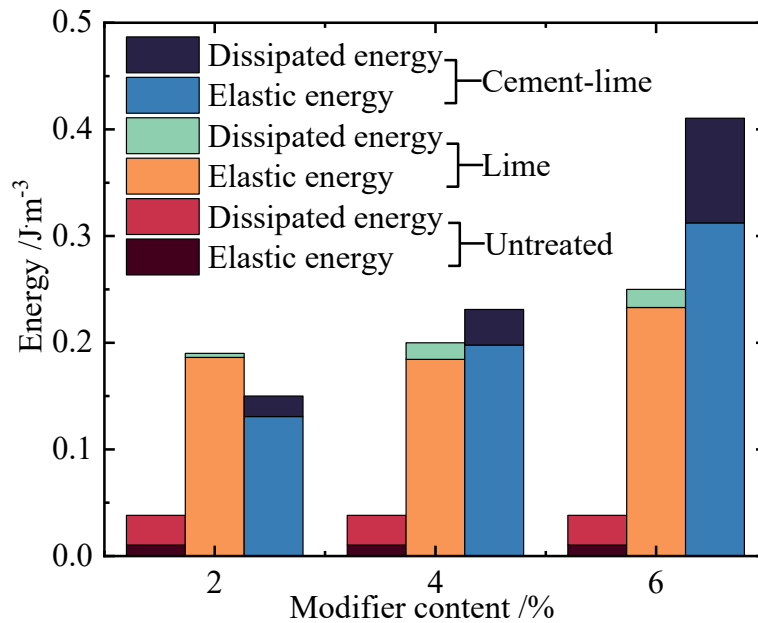


Fig. 12 Evolution of energy with different modification content before and after modification

4.3 The microstructure of the modified red mudstone fill material

To fulfil the comprehension of the experimental outcomes and deepen the interpretation of the behaviour observed during the UCS testing, Scanning Electron Microscopy (SEM) analyses were systematically performed on untreated, lime stabilised, and cement-lime modified specimens. This approach enabled a thorough assessment of the microstructural changes, thereby deepening the overall understanding of the experimental results (Yuan et al. 2016; Liu et al. 2016).

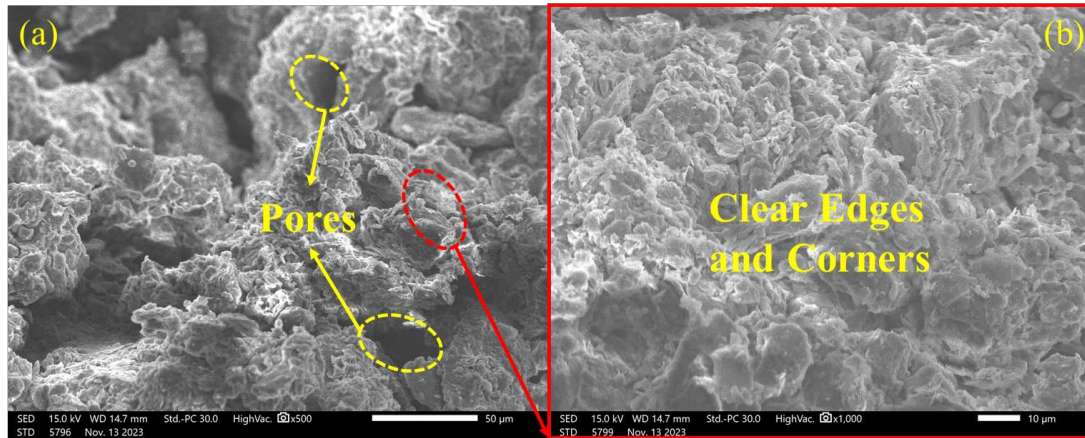


Fig. 13 Microstructure of red mudstone fill material before saturation

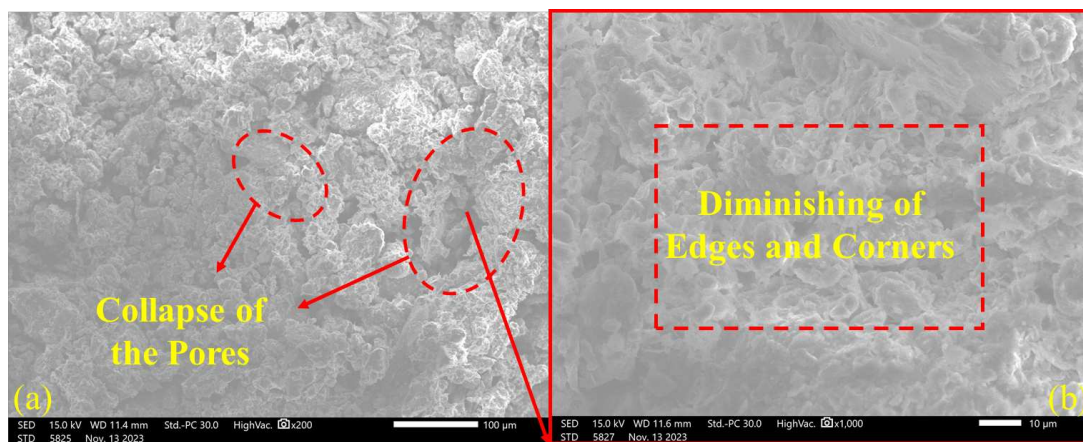


Fig. 14 Microstructure of red mudstone fill material in a saturated state

Fig. 14 presents a detailed morphological analysis of untreated red mudstone before saturation, showcasing sharply demarcated edges and corners of the constituent particles, facilitating clear differentiation. Furthermore, a profusion of distinct pores is discernible within the inter-particle matrix. Conversely, upon hydration of the specimen to saturation, a notable transformation occurs: the prominent inter-particle pores diminish, and the once sharply defined edges and corners become blurred, as evident in Fig. 15(1) and (2).

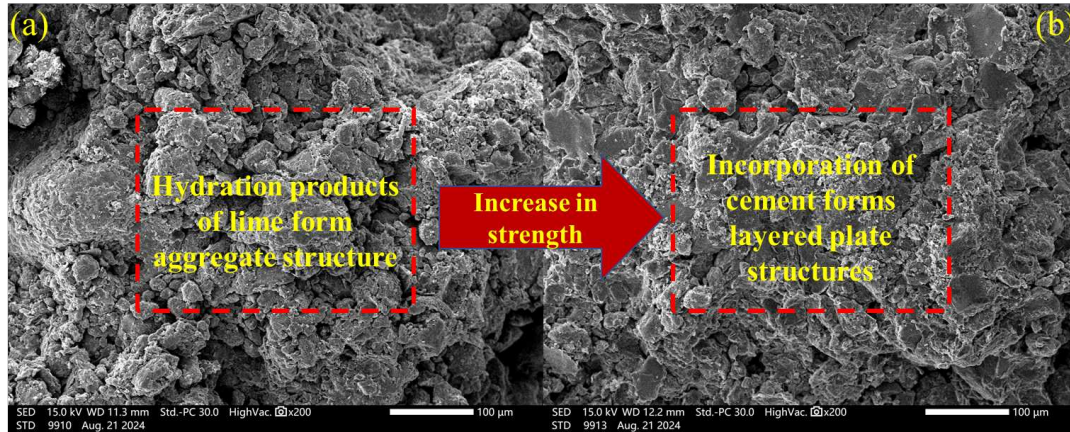


Fig. 15 Microstructure of modified red mudstone fill material in saturated state (a) Lime stabilised (b) Cement-lime modified

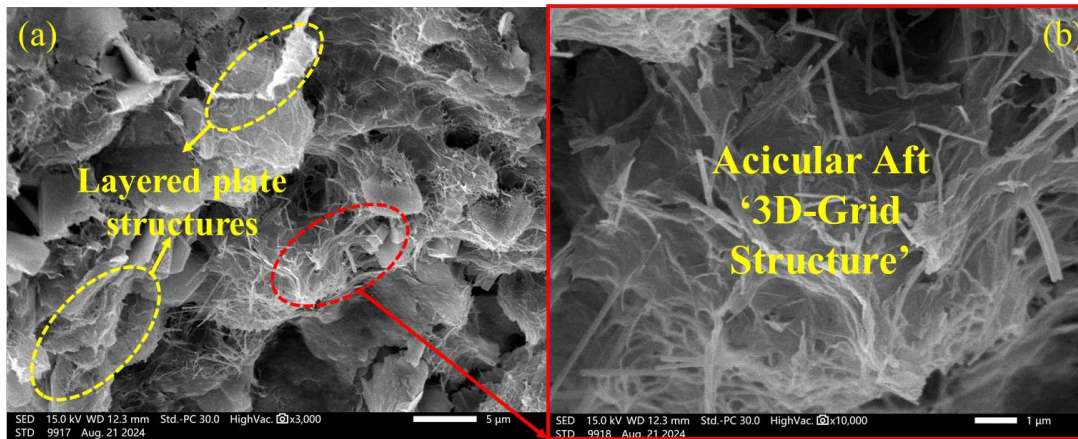


Fig. 16 Microscopic modification mechanism

Fig. 16 demonstrates the morphology of the modified red mudstone under saturated state. After lime stabilisation, a pronounced aggregate structure emerges, accompanied by the appearance of cementitious bodies between these aggregates. Furthermore, the incorporation of cement leads to the formation of distinct layered plate structures, significantly contributing to the enhancement of strength. To reveal the microscopic modification mechanisms, a high-magnification SEM analysis is conducted (see Fig. 17). Upon the addition of lime and cement, the expansive properties could be effectively mitigated. Simultaneously, the interplay between cement-lime and the fill material fosters the formation of needle-like calcium cementations among aggregates. This structural reinforcement not only tightens the aggregates but also markedly strengthens the overall stability of the fill material structure. Consequently, even when the specimen is saturated, the reduction in strength and modulus remains relatively limited compared

with the untreated red mudstone, particularly when the initial dry density of the fill material is low and its structure is relatively loose, underscoring the persistence of this advantageous characteristic.

The effectiveness of SEM image analysis can be enhanced by using Image Pro Plus 6.0 software(Yang et al. 2019; Wang et al. 2020), which aids in a quantitative evaluation of void fraction relative to the total pore area ratio obtained from the SEM images(Li et al. 2019, 2021). Herein, the pore area ratio could be defined as:

$$PAR = \frac{A_{pore}}{A_{total}} \times 100\% \quad (3)$$

where A_{pore} is the pore area and the A_{total} is the total area of image. To ensure the accuracy of the results, the SEM images of different samples under the same conditions were analysed and the outcomes were averaged. Notably, the pore area ratio (PAR) calculated for the untreated red mudstone fill material was 0.4998, which closely aligns with the target porosity ratio of the specimens used for SEM which is 0.4944. This could emphasise the reliability of IPP 6.0 for precise pore space characterisation.

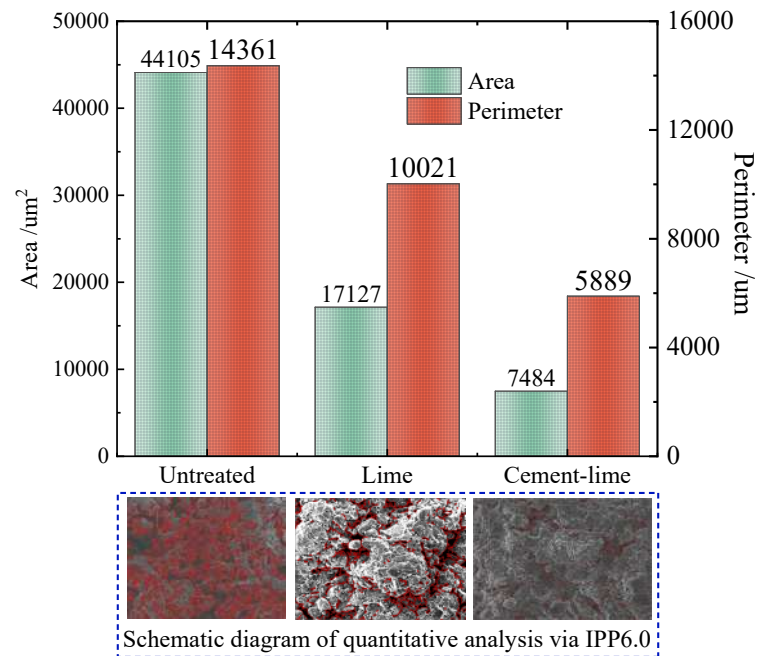


Fig. 17 Evolution of the pore area and the pore perimeter before and after modification

Fig. 18 presents the evolution of the pore area and the pore perimeter before and after the modification. It can be seen that the addition of lime could significantly reduce the area and the perimeter of the pores within the specimens. The hydration products (see Fig. 16 and 22) could fill the existing pores which is consistent with the earlier qualitative analysis. Moreover, the incorporation of cement further fills the pores, creating a more compact structure of the red mudstone.

5. Conclusions

This study investigates the influence of dry density and modifier content on the static properties of saturated red mudstone fill material, lime stabilised, and cement-lime modified filler, employing a series of UCS tests and SEM analysis. The microstructural modification mechanisms are revealed, and the macro-mechanical behaviour is interpreted from an energy perspective. The primary conclusions are as follows:

(1) The unconfined compressive strength and elastic modulus of lime stabilised specimens increase with the increase of dry density and modifier content, representing a significant improvement over untreated red mudstone fill material. This suggests that lime stabilisation could effectively mitigate the water sensitivity of red mudstone. When cement is incorporated into the 4% lime stabilised filler, both peak strength and elastic modulus are further enhanced, accompanied by a more significant tendency towards brittle failure.

(2) The modulus characteristics of the fill material exhibit a notable nonlinear degradation trend as the shear stress increases. Additionally, dry density and modifier content have a substantial impact on the modulus degradation (i.e., structural damage) of red mudstone fill material. Specifically, as dry density and modifier content increase, modulus degradation improves, with the tangent modulus dropping to 60% of its initial value at shear stress levels of 0.74, 0.92 and 0.99 for untreated soil, lime stabilised filler, and cement-lime modified filler, respectively.

(3) Explaining the macro-mechanical behaviour via energy evolution patterns, both elastic and dissipated energies of red mudstone fill material and its modified filler increase with increasing dry density, stemming from tighter arrangements of soil

particles. This arrangement not only strengthens the soil mass but also intensifies inter-particle interlocking and friction during loading, leading to gradual energy dissipation through these microscopic interactions. Moreover, with the increase of modifier content, the total energy, including elastic and dissipated energy, increases. Notably, with a cement content of 6%, the total energy exceeds that of the untreated material by more than 8 times, indicating a significant increase in macroscopic brittleness. This may make the material more prone to sudden fracture under external forces.

(4) At the microstructural level, the reaction between modifier and expansive minerals inhibits the water sensitivity of red mudstone. The formation of needle-like and platy hydration products significantly enhances strength and overall stability, mitigating modulus degradation under saturated conditions. This advantageous behaviour persists even in loosely structured materials. Moreover, the hydration products from lime and cement significantly fill the pores, thereby decreasing pore size and creating a denser structure, as verified by IPP 6.0.

This study delivers essential theoretical insights for railway construction in red bed regions of Southwest China, aligning with the broader initiative to accelerate high-speed rail development. This is crucial for meeting the stringent subgrade stability demands required by higher train speeds. However, the current research does not cover the effects of curing age of the specimens or the dynamic loading from high-speed trains. Future investigations will focus on the impact of curing age and high-frequency train loads, aiming to deepen understanding of the long-term performance and durability of the modified red mudstone subgrade under accelerated conditions.

Statements and Declarations

Funding

Partial financial support was received from Natural Science Foundation of China (No. 52008355, No. 52078432 and No. 52478475) and the funding of China Academy of Railway Science Group Co., LTD (NO. 2023YJ377)

Competing interests

The authors have no relevant financial or non-financial interests to disclose.

Author contributions

All authors contributed to the study conception and design. Material preparation, data collection and analysis were performed by Jiahang Xu, Jie Ma, Xianfeng Liu and Shengyang Yuan. The first draft of the manuscript was written by Jiahang Xu, Shengyang Yuan and Xianfeng Liu, and all authors commented on previous versions of the manuscript. All authors read and approved the final manuscript.

5 References

- Aldaoood A, Bouasker M, Al-Mukhtar M (2014) Soil–water characteristic curve of lime treated gypseous soil. *Appl Clay Sci* 102:128–138. <https://doi.org/10.1016/j.clay.2014.09.024>
- Al-Mukhtar M, Lasledj A, Alcover J-F (2010) Behaviour and mineralogy changes in lime-treated expansive soil at 20°C. *Appl Clay Sci* 50:191–198. <https://doi.org/10.1016/j.clay.2010.07.023>
- Alvarez JI, Fernández JM, Navarro-Blasco I, et al (2013) Microstructural consequences of nanosilica addition on aerial lime binding materials: Influence of different drying conditions. *Mater Charact* 80:36–49. <https://doi.org/10.1016/j.matchar.2013.03.006>
- Ayers LEW, Sullivan WG, Howard IL, Carey AS (2024) Characterizing Lime- and Cement-Treated Soil with the PM Device at a Full-Scale Pavement Test Track. *J Mater Civ Eng* 36:04023620. <https://doi.org/10.1061/JMCEE7.MTENG-16670>
- Chen K, Liu X-F, Yuan S-Y, et al (2022) Shakedown behavior of saturated weathered red mudstone. *Soil Dyn Earthq Eng* 162:107497. <https://doi.org/10.1016/j.soildyn.2022.107497>
- Chen K, Yuan S, Pan S, et al (2023) Energy-based insight into characterization of shakedown behavior of fully weathered red mudstone. *Soils Found* 63:101360. <https://doi.org/10.1016/j.sandf.2023.101360>
- Chen W, Jiang G, Zhao H, et al (2014) Analysis of nonlinear settlement for an unsaturated soil under stage continuous loading. *J Cent South Univ* 21:4690–4697. <https://doi.org/10.1007/s11771-014-2478-2>

China Railway First Survey and Design Institute Group Co., Ltd. (2005) Code for design on subgrade of railway

China Railway First Survey and Design Institute Group Co., LTD, China Railway Third Survey and Design Institute Group Co., LTD., China Railway Fifth Survey and Design Institute Group Co., LTD., et al (2023) Code for Soil Test of Railway Engineering

GhavamShirazi S, Bilsel H (2021) Characterization of volume change and strength behavior of micro-silica and lime-stabilized Cyprus clay. *Acta Geotech* 16:. <https://doi.org/10.1007/s11440-020-01060-1>

Hu A, Jiang G, Wei Y, Wang Z (2010) Dynamic Triaxial Experimental Study on Red Mudstone Filling for Mixed Passenger and Freight Railway with the Speed of 200 km/h. *J China Railw Soc* 32:120–123

Huang K, Wang H, Huang K (2023) Freeze–Thaw Cycle Effects on the Energy Dissipation and Strength Characteristics of Alkali Metakaolin-Modified Cement Soil under Impact Loading. *Water* 15:730. <https://doi.org/10.3390/w15040730>

Kong X, Jiang G, Zou Z, Li A (2013) DYNAMIC CHARACTERISTICS AND PAVEMENT PERFORMANCE OF RED MUDSTONE SUBJECTED TO CYCLIC LOADING. *Chin J Rock Mech Eng* 32:1813–1819

Li J, Wang X, Zhang Y, et al (2021) A Mechanism Study of Trial Loess Reinforced by F1 Ionic Soil Stabilizer on Curing Mechanism and Strength Characteristics. *Cailiao DaobaoMaterials Rep* 35:6100–6106. <https://doi.org/10.11896/cldb.20050034>

Li X-A, Li L, Song Y, et al (2019) Characterization of the mechanisms underlying loess collapsibility for land-creation project in Shaanxi Province, China—a study from a micro perspective. *Eng Geol* 249:77–88. <https://doi.org/10.1016/j.enggeo.2018.12.024>

Liu X, Zhang C, Yuan S, et al (2016) Effect of High Temperature on Mineralogy, Microstructure, Shear Stiffness and Tensile Strength of Two Australian Mudstones. *Rock Mech Rock Eng* 49:3513–3524. <https://doi.org/10.1007/s00603-016-1024-y>

Liu X-F, Chen K, Yuan S-Y, et al (2024) Experimental study on the small strain stiffness-strength of a fully weathered red mudstone. *Constr Build Mater* 438:137058. <https://doi.org/10.1016/j.conbuildmat.2024.137058>

Ma J, Liu X, Yuan S, et al (2024) Multi-scale investigation on curing time effect of

lime stabilized red mudstone as fill material for high-speed railway subgrade. *Constr Build Mater* 443:137749. <https://doi.org/10.1016/j.conbuildmat.2024.137749>

Maubec N, Deneele D, Ouvrard G (2017) Influence of the clay type on the strength evolution of lime treated material. *Appl Clay Sci* 137:107–114. <https://doi.org/10.1016/j.clay.2016.11.033>

Ministry of Railways of the People's Republic of China (2015) TB 10621-2014 Code for design of high speed railway. China Railway Publishing House, Beijing

Onyelowe K, Moghal A, Ebid A, et al (2024) Estimating the strength of soil stabilized with cement and lime at optimal compaction using ensemble-based multiple machine learning. *Sci Rep* 14:. <https://doi.org/10.1038/s41598-024-66295-4>

Tran TD, Cui Y-J, Tang AM, et al (2014) Effects of lime treatment on the microstructure and hydraulic conductivity of Héricourt clay. *J Rock Mech Geotech Eng* 6:399–404

Wang D, Yang C, Cheng G, et al (2020) Experimental Study on Pore Water Pressure and Microstructures of Silty Clay Under Freeze-Thaw Cycles. In: Petriaev A, Konon A (eds) *TRANSPORTATION SOIL ENGINEERING IN COLD REGIONS, VOL 2*. Springer-Verlag Singapore Pte Ltd, Singapore, pp 239–254

Wang S, Shi K, Chen Y, et al (2023a) Analysis of Strength Characteristics and Energy Dissipation of Improved-Subgrade Soil of High-Speed Railway above Mined-Out Areas. *Teh Vjesn* 30:256–264. <https://doi.org/10.17559/TV-20220502051049>

Wang W, Lv B, Zhang C, et al (2023b) Mechanical and micro-structure characteristics of cement-treated expansive soil admixed with nano-MgO. *Bull Eng Geol Environ* 82:48. <https://doi.org/10.1007/s10064-022-03055-6>

Wang Y, Cui Y, Tang A-M, et al (2015) Effects of aggregate size on water retention capacity and microstructure of lime-treated silty soil. *Géotechnique Lett* 5:269–274. <https://doi.org/10.1680/jgele.15.00127>

Wang Z, Jiang G, Wei Y, Hu A (2008) Experimental study on dynamic performance of red mudstone subgrade of Dazhou-Chengdu Railway under cyclic loads. *Chin J Geotech Eng* 30:1888–1893

Wang Z, Jiang G, Wei Y, Hu A (2010) Experimental study of cyclic loading for

subgrade bed of high speed railway. *Rock Soil Mech* 31:760–764.
<https://doi.org/10.16285/j.rsm.2010.03.015>

Wassie T, Demir G (2024) Mechanical Strength and Microstructure of Soft Soil Stabilized with Cement, Lime, and Metakaolin-Based Geopolymer Stabilizers. *Adv Civ Eng* 2024:11. <https://doi.org/10.1155/2024/6613742>

Xu J, Liu X, Ma J, et al (2024a) Multiscale investigation on the shear behaviour of lime-basalt fibre modified red mudstone as fill material for high-speed railway. *Constr Build Mater* 456:138961. <https://doi.org/10.1016/j.conbuildmat.2024.138961>

Xu J, Liu X, Ma J, Yuan S (2024b) Shear behavior of basalt fiber modified compacted red mudstone as subgrade fill material. *IOP Conf Ser Earth Environ Sci* 1332:012013. <https://doi.org/10.1088/1755-1315/1332/1/012013>

Yang X, Wang J, Zhu C, et al (2019) Effect of wetting and drying cycles on microstructure of rock based on SEM. *Environ EARTH Sci* 78:183. <https://doi.org/10.1007/s12665-019-8191-6>

Yuan S, Liu X, Sloan SW, Buzzi OP (2016) Multi-scale characterization of swelling behaviour of compacted Maryland clay. *Acta Geotech* 11:789–804. <https://doi.org/10.1007/s11440-016-0457-5>

Zhan Y, Jiang G, Hu A, Wei Y (2009) Study of dynamic response of pile-plank embankment of ballastless track based on field test in Suining-Chongqing High-speed Railway. *Rock Soil Mech* 30:832–835. <https://doi.org/10.16285/j.rsm.2009.03.007>

Zhang C, Jiang G, Liu X, Buzzi O (2016) Arching in geogrid-reinforced pile-supported embankments over silty clay of medium compressibility: Field data and analytical solution. *Comput Geotech* 77:11–25. <https://doi.org/10.1016/j.compgeo.2016.03.007>

Zhang C, Jiang G, Su L, Liu W (2018) Dynamic behaviour of weathered red mudstone in Sichuan (China) under triaxial cyclic loading. *J Mt Sci* 15:1789–1806. <https://doi.org/10.1007/s11629-017-4756-6>